

## Theoretical Studies on the Addition Reactions of Ketene with NH<sub>3</sub> in the Gas Phase and in Non-Aqueous Solutions

Chang Kon Kim, Kyung A Lee, Junxian Chen, Hai Whang Lee, Bon-Su Lee, and Chan Kyung Kim\*

Department of Chemistry, Inha University, Incheon 402-751, Korea. \*E-mail: kckyung@inha.ac.kr

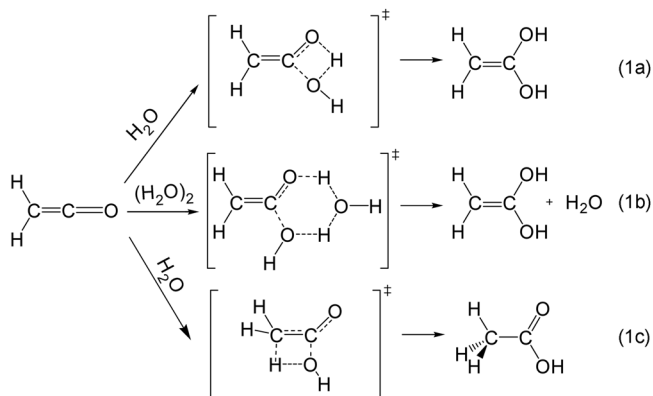
Received April 11, 2008

Theoretical studies on the un-catalyzed and catalyzed aminations of ketene with NH<sub>3</sub> and (NH<sub>3</sub>)<sub>2</sub>, respectively, were studied using MP2 and hybrid density functional theory of B3LYP at the 6-31+G(d,p) and 6-311+G(3df,2p) basis sets in the gas phase and in benzene and acetonitrile solvents. In the gas phase reaction, the un-catalyzed mechanism was the same as those previously reported by others. The catalyzed mechanism, however, was more complicated than expected requiring three transition states for the complete description of the C=O addition pathways. In the un-catalyzed amination, rate determining step was the breakdown of enol amide but in the catalyzed reaction, it was changed to the formation of enol amide, which was contradictory to the previous findings. Starting from the gas-phase structures, all structures were re-optimized using the CPCM method in solvent medium. In a high dielectric medium, acetonitrile, a zwitterions formed from the reaction of CH<sub>2</sub>=C=O with (NH<sub>3</sub>)<sub>2</sub>, **I(d)**, exists as a genuine minimum but other zwitterions, **I(m)** in acetonitrile and **I(d)** in benzene become unstable when ZPE corrected energies are used. Structural and energetic changes induced by solvation were considered in detail. Lowering of the activation energy by introducing additional NH<sub>3</sub> molecule amounted to *ca.* -20 ~ -25 kcal/mol, which made catalyzed reaction more facile than un-catalyzed one.

**Key Words** : Amination of ketene, Solvent effect, CPCM optimization, Basis set superposition error

### Introduction

Ketene is a well-known reactive species, and its structural characteristics and reactions have been extensively studied both experimentally<sup>1</sup> and theoretically.<sup>1b,2</sup> In particular, the hydration of ketene, the reverse of the dehydration of acetic acid, has been considered a prototypical reaction, which in solution, proceeds by addition of one or two H<sub>2</sub>O molecules to the C=O bond to form an enol intermediate, eqs. (1a) and (1b), and not addition to the C=C bond to form the carboxylic acid directly, eq. (1c). There is theoretical evidence that the addition of (H<sub>2</sub>O)<sub>2</sub>, eq. (1b), is more favorable than that of H<sub>2</sub>O, eq. (1a).<sup>2c</sup>



Amination of ketene is also of synthetic interest. In early experimental<sup>3</sup> and theoretical studies,<sup>4</sup> this reaction was reported to proceed more favorably by addition to the C=C bond rather than the C=O bond, in contrast to the hydration

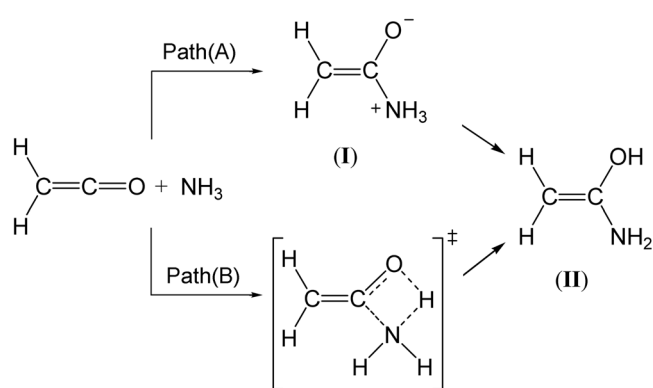
reaction mentioned above. However, more recent work in the gas phase<sup>5</sup> and in solution phase<sup>6</sup> has found addition to the C=O bond to be more favorable than addition to the C=C bond. Amination of ketene is therefore expected to be analogous to hydration.

Two different mechanisms have been proposed to explain the results of kinetic studies. Wagner and co-workers have observed linear dependence of the rate constant on the concentration of amine in the reaction of phenyl ketene with diethylamine in acetonitrile solution, eq. (2),<sup>5b,c</sup> suggesting that only one amine molecule is present in the rate-limiting step. In contrast, Satchell and co-workers have found that the reactions of dimethyl ketene and diphenyl ketene with anilines follow the rate law shown in eq. (3) in benzene and in ether.<sup>3,7</sup> This implies that the reaction proceeds competitively *via* two different amine species.<sup>8</sup> Such mechanisms are now established by theoretical studies of the hydration of ketones,<sup>9</sup> the hydration and ammonolysis of  $\beta$ -lactams,<sup>10</sup> and the hydration<sup>1,2</sup> and amination<sup>5a,6</sup> of ketenes. A second amine molecule acts as a bifunctional catalyst to lower activation energies.

$$\text{Rate} = k_1[\text{Amine}][\text{Ketene}] \quad (2)$$

$$\text{Rate} = (k_1[\text{Amine}] + k_2[\text{Amine}]^2)[\text{Ketene}] \quad (3)$$

On the whole, direct comparison of experiment and theory has not been possible because most of the theoretical work refers to the gas phase. Recent developments in computational methodology enable us to study such reactions in solution using continuum models.<sup>11</sup> In earlier work, the solvation energy was estimated by single-point calculations



on gas-phase optimized geometries, but geometry optimization of stationary points in a solvent has now become possible and several such studies have begun to appear in the literature.<sup>12</sup> The work of Ngugen, and coworkers is especially noteworthy.<sup>6</sup> They examined the amination of ketene in water solvent using the Onsager SCRF, PCM and SCI-PCM electrostatic continuum solvation models by reoptimization of gas-phase stationary points, and found that the profile of the reaction is not changed significantly.

In the gas phase, the formation of a zwitterionic intermediate is unlikely because of its intrinsic instability. In solution, however, such species can be stabilized by solvation and studies should be therefore expanded to take these species into account. Zwitterions, formed from the reaction of ketene with tertiary amines,<sup>13</sup> have in fact been identified experimentally by UV and IR by use of time-resolved laser flash photolyses<sup>14</sup> and theoretically in AM1<sup>15</sup> or BLYP calculations.<sup>16</sup>

The addition of  $\text{NH}_3$  or a primary amine to ketene can proceed by two different pathways, stepwise *via* a ketene-nucleophile zwitterion, (**I**), or concerted *via* a neutral four-center cyclic transition state as shown in Scheme 1. Experimentally, evidence for the zwitterion (**I**) has been reported by UV/VIS spectroscopic<sup>17</sup> and IR studies.<sup>18</sup> Thus Wagner

and co-workers observed a transient intermediate with an IR band at  $1680\text{ cm}^{-1}$  during the amination of ketene with diethylamine.<sup>5b</sup> However, it is difficult to determine unambiguously whether (**I**) or (**II**) is the initial intermediate, because the characteristic IR absorption of the zwitterionic ylide (**I**) is similar to the IR absorption for C=C bond stretching of the enol amide (**II**). Since none of the previous theoretical studies has considered a zwitterion as a transient intermediate in the reaction of ketene with  $\text{NH}_3$  or a primary amine and the stability of the zwitterion (**I**) should depend upon the reaction medium, additional theoretical studies are needed.

In the present work, the amination of ketene by  $\text{NH}_3$  and the  $(\text{NH}_3)_2$  has been examined theoretically in the gas phase and in benzene and acetonitrile.

### Calculations

For the gas-phase reactions, all stationary points were optimized fully at MP2/6-31+G(d,p), B3LYP/6-31+G(d,p) and B3LYP/6-311+G(3df,2p) levels of theory and characterized by frequency calculations. Reactants, intermediates and products exhibited no, and transition structures exhibited one imaginary frequency. Solvent effects in benzene (dielectric constant = 2.247) and acetonitrile (dielectric constant = 36.64) were considered by using the CPCM methodology<sup>19</sup> at CPCM-B3LYP/6-31+G(d,p) and CPCM-B3LYP/6-311+G(3df,2p) levels. Geometries and energies in solution were also fully optimized with the OPT=LOOSE option to achieve convergence,<sup>20</sup> and characterized by frequency calculations at each level. Reactant complexes (**RC**) and product complexes (**PC**) are not considered in detail because they do not exist in solution. All calculations were performed with the Gaussian 98 program.<sup>21</sup> Intrinsic reaction coordinate (IRC) calculations<sup>22</sup> were performed at MP2/6-31+G(d,p) and B3LYP/6-31+G(d,p) levels of theory to confirm direct connection between transition structures and minima on both sides of the potential energy surfaces. The

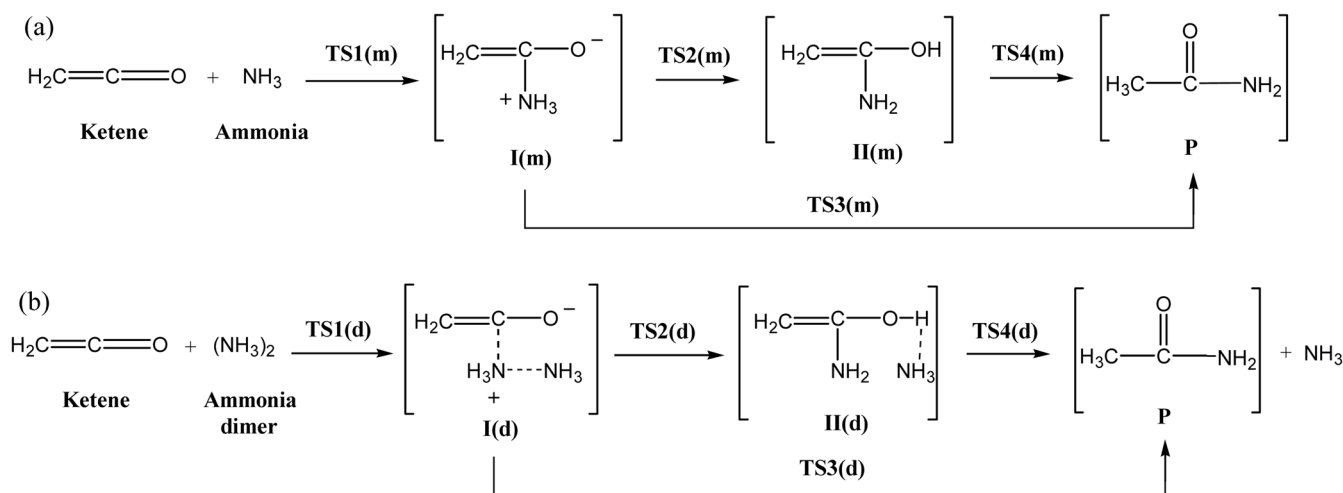


**Figure 1.** Schematic diagram for the addition reactions of  $\text{NH}_3$  (a) and  $\text{NH}_3$  dimer (b) to ketene. (m) refers to the reaction with monomer and (d) refers to the reaction with dimer. Four transition structures were found in (b) but some do not exist in the case of (a). See text for details.

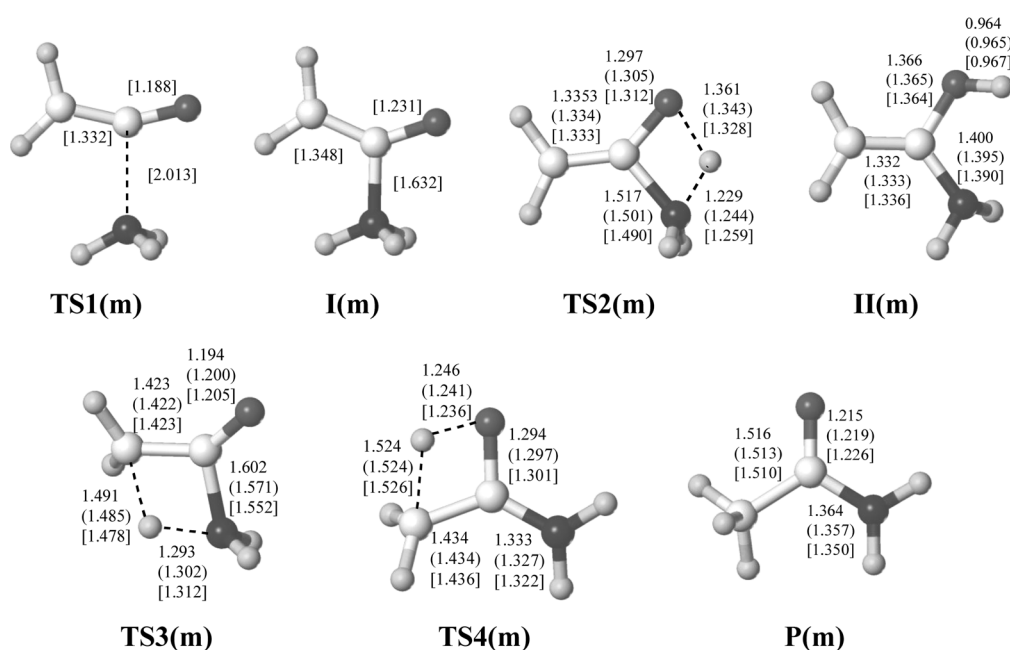


**Figure 2.** Optimized stationary structures for the addition reaction of  $\text{NH}_3$  monomer to ketene at the B3LYP/6-311+G(3df,2p) level. Geometrical parameters shown with each structure refer to the gas-phase, benzene (in parentheses) and acetonitrile (in square brackets). Bond lengths are in Å.

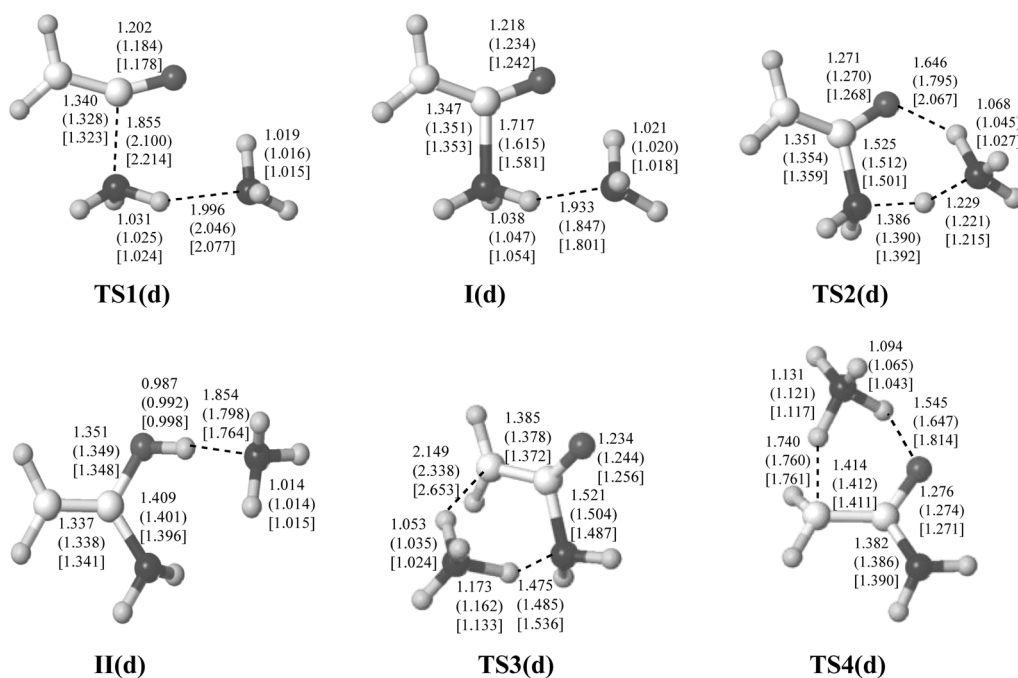


**Figure 3.** Optimized stationary structures for the addition of  $\text{NH}_3$  dimer to ketene at the B3LYP/6-311+G(3df,2p) level. Geometrical parameters shown with each structure refer to the gas-phase, benzene (in parentheses) and acetonitrile (in square brackets). Bond lengths are in Å.

different reaction sequences are summarized in Figure 1 and the optimized stationary structures are shown in Figures 2 and 3.

## Results and Discussion

**The Gas-Phase Aminations of Ketene.** According to the gas-phase computations of Sung and Tidwell,<sup>5a</sup> amination of

ketene by attack on the C=O bond to give an initial enol amide is preferred over addition to the C=C bond to produce an amide directly. These workers also found amination by dimeric  $(\text{NH}_3)_2$  to be more favorable than amination by  $\text{NH}_3$ . The same results were obtained at the QCISD/6-311+G(d,p)/MP2/6-31G(d,p) theoretical level.<sup>6</sup>

The zero-point energy (ZPE) corrected activation ( $\Delta E_{\text{ZPE}}^\ddagger$ ) and reaction ( $\Delta E_{\text{ZPE}}^0$ ) energy changes for the amination of

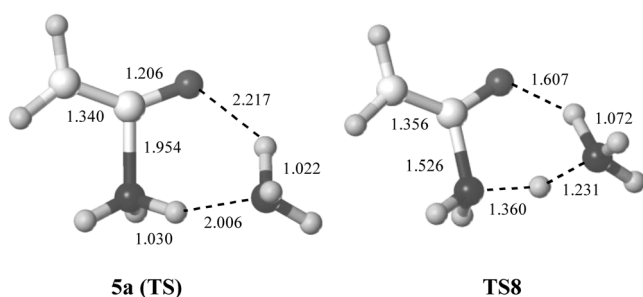
**Table 1.** ZPE corrected activation and reaction energy changes (in kcal mol<sup>-1</sup>) relative to the separated reactants for the amination process of ketene with NH<sub>3</sub>

Process	Phase	Level	Reactant	TS	Product
Ketene + NH <sub>3</sub> → <b>I(m)</b>	Acetonitrile	B3LYP/6-31+G(d,p)	0.00	<b>TS1(m)</b> 3.64	<b>I(m)</b> 7.21 <sup>a</sup>
		B3LYP/6-311+G(3df,2p)	0.00	6.03	6.70
Ketene + NH <sub>3</sub> (C=O addition)	Gas	B3LYP/6-31+G(d,p)	0.00	<b>TS2(m)</b> 28.81	<b>II(m)</b> -5.31
		B3LYP/6-311+G(3df,2p)	0.00	32.63	-2.44
		MP2/6-31+G(d,p)	0.00	28.67	-6.32
	Benzene	B3LYP/6-31+G(d,p)	0.00	25.85	-6.93
		B3LYP/6-311+G(3df,2p)	0.00	29.82	-4.08
	Acetonitrile	B3LYP/6-31+G(d,p)	0.00	23.74	-8.22
		B3LYP/6-311+G(3df,2p)	0.00	27.60	-5.59
	Ketene + NH <sub>3</sub> (C=C addition)	Gas	B3LYP/6-31+G(d,p)	0.00	<b>TS3(m)</b> 39.09
B3LYP/6-311+G(3df,2p)			0.00	42.95	-28.67
MP2/6-31+G(d,p)			0.00	39.71	-34.78
Benzene		B3LYP/6-31+G(d,p)	0.00	37.14	-35.38
		B3LYP/6-311+G(3df,2p)	0.00	41.00	-31.10
Acetonitrile		B3LYP/6-31+G(d,p)	0.00	35.87	-37.11
		B3LYP/6-311+G(3df,2p)	0.00	39.56	-33.00
<b>II(m)</b> → <b>P</b> (uncatalyzed)		Gas	B3LYP/6-31+G(d,p)	-5.31	<b>TS4(m)</b> 30.40
	B3LYP/6-311+G(3df,2p)		-2.44	34.48	-28.67
	MP2/6-31+G(d,p)		-6.32	31.52	-34.78
	Benzene	B3LYP/6-31+G(d,p)	-6.93	28.27	-35.38
		B3LYP/6-311+G(3df,2p)	-4.08	32.32	-31.10
	Acetonitrile	B3LYP/6-31+G(d,p)	-8.22	26.97	-37.11
		B3LYP/6-311+G(3df,2p)	-5.59	30.78	-33.00

<sup>a</sup>This structure has one imaginary frequency at this level of theory. We use ZPE obtained at B3LYP/6-311+G(3df,2p) level instead.

ketene obtained in the present work are summarized in Tables 1 and 2. The gas-phase results for NH<sub>3</sub> addition reported in Table 1 are consistent with those reported previously, but the results for (NH<sub>3</sub>)<sub>2</sub> addition reported in Table 2 are not.

In the previous works,<sup>5a,6</sup> different transition structures were found for the C=O addition step **5a(TS)**<sup>5a</sup> at MP2/6-



31G(d) and **TS8**<sup>6</sup> at MP2/6-31G(d,p) levels. There is little bond formation and cleavage in **5a(TS)** but both are well advanced in **TS8**. The difference can be understood upon inspection of **TS1(d)** and **TS2(d)** shown in Figure 3. The former refers to the addition of NH<sub>3</sub> hydrogen-bonded to the catalytic NH<sub>3</sub>, its geometrical parameters are similar to those

of **5a(TS)**. Likewise, the geometrical parameters of **TS8** are similar to those of **TS2(d)**. It seems that not all transition structures were located in the previous works, possibly because examination of the intrinsic reaction coordinate (IRC) to search for minima present on both sides of the PES was not performed. IRC calculations on **TS1(d)** and **TS2(d)** at MP2/6-31+G(d,p) and B3LYP/6-31+G(d,p) levels show that **TS1(d)** is connected to **RC(d)** and **I(d)**, and **TS2(d)** is connected to **I(d)** and **II(d)**. This means that **TS1(d)** and **TS2(d)** are genuine transition structures for addition to the C=O bond. The former is the saddle point leading to the zwitterion, **I(d)**, and the latter leads to the enol amide intermediate, **II(d)**. The zwitterionic character of **I(d)** is seen in its important charge distribution: in the separated reactants the MP2/6-31+G(d) NBO<sup>23</sup> group charges on oxygen and the attacking NH<sub>3</sub> are -0.413 and -0.015 electrons, respectively, the corresponding charges in **I(d)** are -0.707 and +0.442 electrons respectively at MP2/6-31+G(d) level.<sup>24</sup>

Inclusion of additional species in the description of the C=O addition step makes the PES more complex - three transition structures and four intermediates are required. Figure 4 depicts the gas-phase and solution-phase potential energy diagrams. The rate-determining step for the gas-phase C=O addition is a cooperative process in which enol

**Table 2.** ZPE corrected activation and reaction energy changes (in kcal mol<sup>-1</sup>) relative to the separated reactants for the amination process of ketene with (NH<sub>3</sub>)<sub>2</sub>

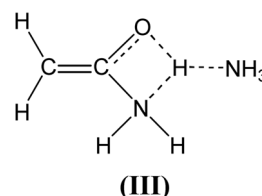
Process	Phase	Level	Reactant	TS	Product	
Ketene + (NH <sub>3</sub> ) <sub>2</sub> → <b>I(d)</b>	Gas	B3LYP/6-31+G(d,p) <sup>a</sup>	0.00	<b>TS1(d)</b> 2.68	<b>I(d)</b> 3.59	
		B3LYP/6-311+G(3df,2p)	0.00	6.37	7.11	
		MP2/6-31+G(d,p)	0.00	1.99	2.50	
		Benzene	B3LYP/6-31+G(d,p)	0.00	1.43	0.61
			B3LYP/6-311+G(3df,2p)	0.00	3.70	3.85
			Acetonitrile	B3LYP/6-31+G(d,p)	0.00	1.75
	B3LYP/6-311+G(3df,2p)	0.00		4.14	1.79	
	<b>TS2(d)</b>	<b>I(d)</b>				
	Ketene + (NH <sub>3</sub> ) <sub>2</sub> (C=O addition)	Gas	B3LYP/6-31+G(d,p)	0.00	9.62	-10.74
			B3LYP/6-311+G(3df,2p)	0.00	14.76	-7.17
			MP2/6-31+G(d,p)	0.00	9.13	-12.41
			Benzene	B3LYP/6-31+G(d,p)	0.00	4.89
B3LYP/6-311+G(3df,2p)				0.00	9.35	-9.62
Acetonitrile				B3LYP/6-31+G(d,p)	0.00	1.16
		B3LYP/6-311+G(3df,2p)	0.00	6.07	-10.40	
		<b>TS3(d)</b>	<b>P(d)+NH<sub>3</sub></b>			
Ketene + (NH <sub>3</sub> ) <sub>2</sub> (C=C addition)		Gas	B3LYP/6-31+G(d,p)	0.00	14.61	-31.01
			B3LYP/6-311+G(3df,2p)	0.00	19.93	-27.53
			MP2/6-31+G(d,p)	0.00	-	-32.39
			Benzene	B3LYP/6-31+G(d,p)	0.00	8.77
	B3LYP/6-311+G(3df,2p)			0.00	13.12	-31.96
	Acetonitrile			B3LYP/6-31+G(d,p)	0.00	3.56
		B3LYP/6-311+G(3df,2p)	0.00	8.38	-33.19	
		<b>I(d)</b>	<b>TS4(d)</b>	<b>P+NH<sub>3</sub></b>		
	<b>I(d)</b> → <b>P</b> +NH <sub>3</sub> (catalyzed)	Gas	B3LYP/6-31+G(d,p)	-10.74	3.70	-31.01
			B3LYP/6-311+G(3df,2p)	-7.17	8.83	-27.53
			MP2/6-31+G(d,p)	-12.41	4.41	-32.39
			Benzene	B3LYP/6-31+G(d,p)	-12.54	0.09
B3LYP/6-311+G(3df,2p)				-9.62	4.27	-31.96
Acetonitrile				B3LYP/6-31+G(d,p)	-13.76	-2.11
		B3LYP/6-311+G(3df,2p)	-10.40	2.06	-33.19	

<sup>a</sup>(NH<sub>3</sub>)<sub>2</sub> has one imaginary frequency. We use ZPE obtained at B3LYP/6-311+G(3df,2p) level instead.

amide **I(d)** from **I(d)** via **TS2(d)**. In the previous studies, reversible addition of NH<sub>3</sub> to CH<sub>2</sub>=C=O was assumed or the rate-determining step was not identified.<sup>6</sup> In contrast, rate-determining formation of enol amide was found in the reactions of phenyl ketene and 2-pyridylketene with (NH<sub>3</sub>)<sub>2</sub>. Table 3 summarizes the data found at B3LYP/6-311+G(3df,2p). Although the electronic energy of **I(d)** is higher than that of **TS1(d)** when the ZPE correction is included, the zwitterion **I(d)** is confirmed as a genuine intermediate by the frequency and IRC calculations.

This inversion of the energies of stationary points arises from the one absence of one vibrational mode in the TS in the region of the flat transition structure.<sup>25</sup> In the gas-phase amination the zwitterionic species **I(d)** could be a transient intermediate or a non-detectable species, despite its apparent identification as a stable intermediate on the electronic energy PES. Consequently whether a zwitterionic mechanism exists in the gas-phase reaction of ammonia dimer with ketene cannot be established.

There is an alternative cooperative process for the dimeric (NH<sub>3</sub>)<sub>2</sub> addition, in which one NH<sub>3</sub> molecule carries out a 4-centered addition to the carbonyl carbon, and the other NH<sub>3</sub> acts as a general base catalyst (see **III**). This structure could not be located in the present work.



**Amination of Ketene in Solution.** The existence of a zwitterion in the gas phase reaction is problematical as noted above. Although a zwitterion is expected to be more stable in solution the Onsager SCRF, PCM and SCI-PCM continuum models are unable to locate a zwitterionic species.<sup>6</sup> In the present work, a zwitterion **I(m)** corresponding to the

**Table 3.** Summary of electronic energies (in a.u.) of stationary species for the un-catalyzed and catalyzed aminations of ketene and imaginary frequency (in  $\text{cm}^{-1}$ ) for the transition structures at B3LYP/6-311+G(3df,2p)

Species	Gas		Benzene		Acetonitrile	
	Energy	Imaginary freq.	Energy	Imaginary freq.	Energy	Imaginary freq.
Ketene	-152.66269	-	-152.66123	-	-152.65970	-
NH <sub>3</sub>	-56.58688	-	-56.58827	-	-56.58870	-
(NH <sub>3</sub> ) <sub>2</sub>	-113.17781	-	-113.17891	-	-113.17951	-
<b>TS1(m)</b>	-	-	-	-	-209.24328	-208
<b>I(m)</b>	-	-	-	-	-209.24518	-
<b>TS1(d)</b>	-265.83679	-133	-265.83807	-186	-265.83654	-186
<b>I(d)</b>	-265.83690	-	-265.84163	-	-265.84471	-
<b>TS2(m)</b>	-209.20079	-1684	-209.20559	-1729	-209.20768	-1770
<b>TS2(d)</b>	-265.82223	-992	-265.82986	-904	-265.83502	-809
<b>II(m)</b>	-209.26147	-	-209.26417	-	-209.26490	-
<b>II(d)</b>	-265.86050	-	-265.86290	-	-265.86390	-
<b>TS3(m)</b>	-209.18270	-1802	-209.18620	-1843	-209.18711	-1882
<b>TS3(d)</b>	-265.81444	-563	-265.82440	-383	-265.83280	-111
<b>TS4(m)</b>	-209.19691	-1975	-209.20058	-1972	-209.20150	-1965
<b>TS4(d)</b>	-265.83193	-625	-265.83863	-442	-265.84224	-328
<b>P</b>	-209.30266	-	-209.30700	-	-209.30871	-

addition of NH<sub>3</sub> to CH<sub>2</sub>=C=O has been found as a stable structure in acetonitrile solvent and found a zwitterion **I(d)** corresponding to the addition of (NH<sub>3</sub>)<sub>2</sub> has been found as a stable intermediate in benzene and in acetonitrile.

As in the gas-phase reaction, the ZPE correction raises the CPCM energy of the intermediate and reverses the relative stabilities of the intermediate and the transition structure leading to this intermediate. Thus **I(m)** is 3.57 kcal mol<sup>-1</sup> higher than **TS1(m)** at ZPE corrected CPCM-B3LYP/6-31+G(d,p) and 0.67 kcal mol<sup>-1</sup> higher than **TS1(m)** at ZPE-corrected CPCM-B3LYP/6-311+G(3df,2p) in acetonitrile. This zwitterion is therefore expected to be unstable.

The relative stabilities of **I(d)** and **TS1(d)** are basis set dependent in benzene solvent, but the zwitterion **I(d)** is a genuine minimum in acetonitrile solvent. The ZPE corrected energy level of **I(d)** is lower than that of **TS1(d)** by 3.70 kcal mol<sup>-1</sup> at CPCM-B3LYP/6-31+G(d,p) and by 2.35 kcal mol<sup>-1</sup> CPCM-B3LYP/6-311+G(3df,2p) levels, respectively. In **I(d)** at B3LYP/6-311+G(3df,2p) the C-N bond length decreases on going from the gas phase (1.717 Å) to benzene (1.615 Å) to acetonitrile (1.581 Å) (Figure 3), suggesting that the zwitterion is stabilized in the more polar solvent.

**Structures.** The optimized stationary structures on the reaction coordinates in the gas phase and in solvents are represented in Figures 2 and 3 for the un-catalyzed and catalyzed reactions with NH<sub>3</sub> and (NH<sub>3</sub>)<sub>2</sub>, respectively. Structural changes can be examined in two ways, by changing the nucleophile from NH<sub>3</sub> to (NH<sub>3</sub>)<sub>2</sub> or by changing the reaction condition from the gas phase to two solvents. In the reaction with NH<sub>3</sub>, three transition structures, **TS2(m)**, **TS3(m)** and **TS4(m)**, which are tightly bound four-membered structures, are located but become looser six-membered structures when additional NH<sub>3</sub> molecule is participated in the reaction system. Changes in geometrical parameters are more com-

plex when the reaction medium is varied. As can be seen in Figures 2 and 3, the C=O bond length becomes longer but the C-N bond length becomes shorter as the solvent dielectric constant increases. For example, the C=O bond length of product acetamide at B3LYP/6-311+G(3df,2p) level is 1.215 Å (gas phase), 1.219 Å (benzene) and 1.226 Å (acetonitrile) but the C-N bond length is 1.364 Å (gas phase), 1.357 Å (benzene) and 1.350 Å (acetonitrile). Such trends in the bond lengths are true for all other stationary species except for **TS1(d)**, **TS2(d)** and **TS4(d)**. Especially the C-N bond length in **TS1(d)** is lengthened by 0.25 Å on going from the gas phase to benzene and further lengthened by 0.11 Å to acetonitrile. These structural changes suggest that **TS1(d)** becomes earlier transition structure due to the enhanced stabilization of **I(d)** in higher dielectric constant medium, which is in accordance with the Hammond postulate.<sup>26</sup>

Substantial bond length changes also occur in the O-H bond between the carbonyl oxygen and the transferring hydrogen from NH<sub>3</sub> at **TS2(d)** and C-H bond between the terminal carbon (C<sup>1</sup>) and the transferring hydrogen at **TS4(d)** as the solvent dielectric constant increases. These bond length changes are much smaller in the reaction with NH<sub>3</sub>, **TS2(m)** and **TS4(m)**. For example, the O-H bond length is shortened by 0.03 Å in **TS2(m)** but is lengthened by 0.42 Å in **TS2(d)** from the gas phase to acetonitrile solvent. This indicates that the solvent effects on the TS structures are larger for reactions with (NH<sub>3</sub>)<sub>2</sub> than with NH<sub>3</sub>.

**Energetics.** The energies reported in Tables 1 and 2 refer to ketene + NH<sub>3</sub> for the un-catalyzed reaction and to ketene + 2 NH<sub>3</sub> for the catalyzed reaction. In such cases, the basis set that describes a transition structure or intermediate is the combination of the basis set of the individual molecules. Since individual reactants are therefore described by a

**Table 4.** Basis set superposition error<sup>a</sup> (BSSE) calculated in the gas phase using eq. (4)

Process	level	BSSE
Ketene + NH <sub>3</sub> → <b>TS2(m)</b>	B3LYP/6-31+G(d,p)	1.58
	B3LYP/6-311+G(3df,2p)	0.58
	MP2/6-31+G(d,p)	7.62
Ketene + 2NH <sub>3</sub> → <b>I(d)</b>	B3LYP/6-31+G(d,p)	2.57
	B3LYP/6-311+G(3df,2p)	0.58
	MP2/6-31+G(d,p)	8.71
Ketene + (NH <sub>3</sub> ) <sub>2</sub> → <b>I(d)</b>	B3LYP/6-31+G(d,p)	1.60
	B3LYP/6-311+G(3df,2p)	0.45
	MP2/6-31+G(d,p)	6.87
2NH <sub>3</sub> → (NH <sub>3</sub> ) <sub>2</sub>	B3LYP/6-31+G(d,p)	0.68
	B3LYP/6-311+G(3df,2p)	0.09
	MP2/6-31+G(d,p)	1.24

<sup>a</sup> in kcal mol<sup>-1</sup>.

smaller basis, their relative energies are artificially too high and it is necessary to correct energy differences by the quantity  $E_{\text{BSSE}}^{\text{B3LYP}}$  where  $E_{\text{BSSE}}^{\text{B3LYP}}$  is the basis set superposition error. We calculated the BSSE correction using eq. (4) for the termolecular reactions of  $A+B+C \rightarrow [ABC]$ , in which  $[ABC]$  can be either a stable complex or a transition structure on the potential energy surface.<sup>27,28</sup>

$$BSSE = (E_A^{ABC} - E_{A(BC)}^{ABC}) + (E_B^{ABC} - E_{B(AC)}^{ABC}) + (E_C^{ABC} - E_{C(AB)}^{ABC}) \quad (4)$$

In eq. 4  $E_A^{ABC}$  and  $E_{A(BC)}^{ABC}$  are the energies of A at the geometry of A in  $[ABC]$  in the absence and presence of the ghost orbitals of BC, respectively. Since such calculations are not applicable to the solvation model, only the gas-phase BSSE corrections are collected in Table 4, which shows that the BSSE is large for MP2 calculations, smaller for DFT calculations, as is normally observed,<sup>29</sup> and almost negligible with 6-311+G(3df,2p) basis set. It seems that B3LYP/6-311+G(3df,2p) can be used as a BSSE-free method.

In this work, we studied the amination of ketene at MP2/6-31+G(d,p) level, which is the same basis set used by Sung and Tidwell<sup>5a</sup> and hybrid density functional method of B3LYP level with same (6-31+G(d,p)) and larger (6-311+G(3df,2p)) basis sets. The  $\Delta E_{\text{ZPE}}^{\ddagger}$  and  $\Delta E_{\text{ZPE}}^{\circ}$  for the gas-phase aminations at B3LYP/6-31+G(d,p) and MP2/6-31+G(d,p) levels are very similar, although the reaction energies at the MP2 level are slightly more favorable by about 1-3 kcal mol<sup>-1</sup>. In contrast, the  $\Delta E_{\text{ZPE}}^{\ddagger}$  and  $\Delta E_{\text{ZPE}}^{\circ}$  at B3LYP/6-311+G(3df,2p) level are much higher by about 4-7 kcal mol<sup>-1</sup> than those obtained at 6-31+G(d,p) basis sets. For instance, the  $\Delta E_{\text{ZPE}}^{\circ}$  for the gas-phase amination with NH<sub>3</sub> [ $\text{CH}_2=\text{C}=\text{O} + \text{NH}_3 \rightarrow \text{CH}_3-\text{C}(=\text{O})\text{NH}_2$ ] is -34.78, -32.99 or -28.67 kcal mol<sup>-1</sup> at MP2/6-31+G(d,p), B3LYP/6-31+G(d,p) and B3LYP/6-311+G(3df,2p) levels, respectively. From the experimental heats of formation,<sup>30</sup> the reaction enthalpy ( $\Delta H^{\circ}$ ) for this process is -31.2 kcal mol<sup>-1</sup>. When the corresponding  $\Delta E_{\text{ZPE}}^{\circ}$  values are converted into reaction enthalpies ( $\Delta H^{\circ}$ ), it becomes -36.3, -34.3 or -30.0 kcal mol<sup>-1</sup> at each level of

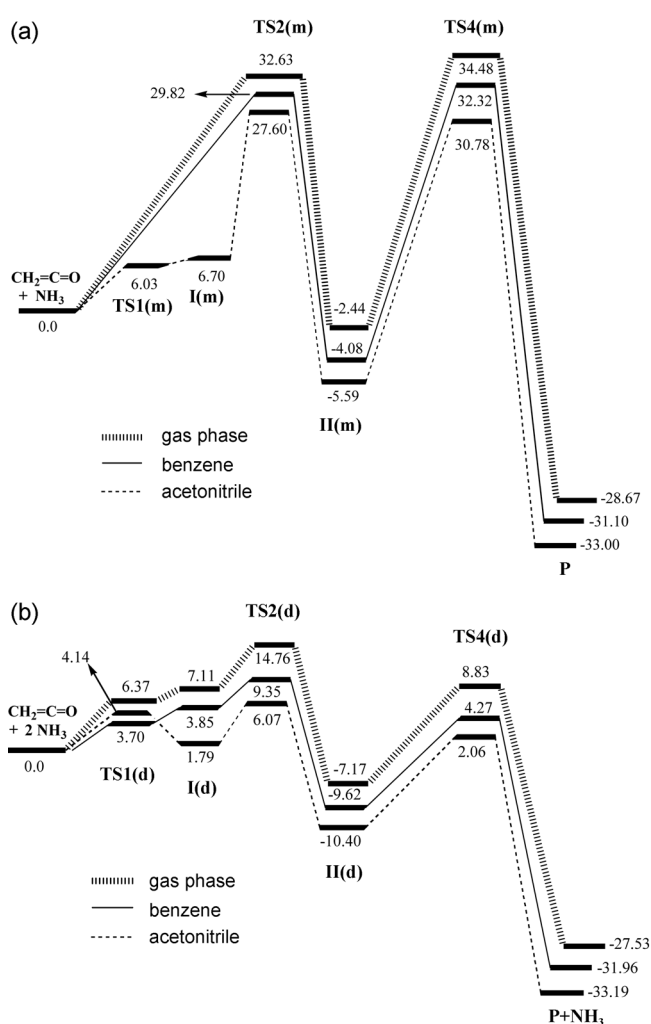


**Figure 4.** Schematic B3LYP/6-31+G(3df,2p) potential energy diagrams (in kcal mol<sup>-1</sup>) in three different phases for the C=O addition pathway (a) with NH<sub>3</sub> and (b) with (NH<sub>3</sub>)<sub>2</sub>. **RC**, **PC** and unfavorable C=C addition pathway *via* **TS3** are not shown for clarity.

theory, which proves that B3LYP/6-311+G(3df,2p) level is more accurate in describing the exothermicity of this reaction. Therefore, further discussions on the energetics will be based on the theoretical values obtained at this level of theory.

In the gas-phase reaction of ketene with monomeric NH<sub>3</sub>, the reaction path through addition to the C=O bond is a stepwise mechanism *via* an intermediate enol amide as shown in Figure 4. The rate-determining step is the second step, which produces product, acetamide, from the enol amide intermediate in all theoretical levels employed, *i.e.*, the  $\Delta E_{\text{ZPE}}^{\ddagger}$  for the second step is higher by 1.85 kcal mol<sup>-1</sup> than that for the first step. On the contrary, the reaction path through addition to the C=C bond proceeds concertedly with 8.46 kcal mol<sup>-1</sup> higher  $\Delta E_{\text{ZPE}}^{\ddagger}$  than that to the C=O bond addition. Gas-phase reaction with (NH<sub>3</sub>)<sub>2</sub> also shows that the C=O addition step is more facile than the C=C bond addition step but mechanistic change is observed in the stepwise C=O addition because the addition step producing the enol amide

**Table 5.** Summary of the solvation energies<sup>a</sup> (in kcal mol<sup>-1</sup>) of all stationary points

	E <sub>sol</sub> (Benzene)	E <sub>sol</sub> (Acetonitrile)
Ketene	0.92	1.87
NH <sub>3</sub>	-0.88	-1.14
(NH <sub>3</sub> ) <sub>2</sub>	-0.69	-1.07
<b>TS1(m)</b>	-	-3.98 <sup>b</sup>
<b>TS1(d)</b>	-0.80	0.16
<b>I(m)</b>	-	-10.95 <sup>b</sup>
<b>I(d)</b>	-2.96	-4.90
<b>TS2(m)</b>	-3.02	-4.32
<b>TS2(d)</b>	-4.79	-8.02
<b>II(m)</b>	-1.69	-2.15
<b>II(d)</b>	-1.51	-2.14
<b>TS3(m)</b>	-2.20	-2.77
<b>TS3(d)</b>	-6.25	-11.52
<b>TS4(m)</b>	-2.30	-2.88
<b>TS4(d)</b>	-4.21	-6.47
<b>P</b>	-2.72	-3.79

<sup>a</sup>solvation energy = E (in solvent) - E (gas phase). <sup>b</sup>Optimized structure in acetonitrile was used to calculate gas-phase energy as a single point energy calculation.

intermediate has higher energy barrier than the breakdown of the enol amide intermediate. Such mechanistic change is possible because highly strained 4-membered **TS4(m)** is changed to a less strained six-membered **TS4(d)** by introducing an additional NH<sub>3</sub>. Therefore, the mechanistic information derived from the false PES in the previous works<sup>5a,6</sup> should be reexamined.

Using the complete PES obtained from this work, it would be interesting to compare the solution phase results with the gas-phase one. The reaction mechanisms in solutions are very similar to those in the gas phase except for the formation of the zwitterion **I(d)** as a genuine intermediate on the ZPE-corrected PES in acetonitrile. Solvent effect can play an important role in controlling the activation barriers or reaction energies depending on the magnitude of solvation energies of all stationary species. If the magnitude of the solvation energy of reactant is greater (smaller) than that of TS, the reaction requires higher (lower) activation energy, and thus becomes unfavorable (favorable). Summary of the solvation energies of all stationary points is represented in Table 5. Solvation energy refers to the difference in energies calculated in solvent medium (benzene or acetonitrile) and in the gas phase. Due to larger dielectric constant, acetonitrile exhibits somewhat larger solvation energy. The solvation energies are in the range +0.9 ~ -6.2 kcal mol<sup>-1</sup> in benzene and +1.9 ~ -11.5 kcal mol<sup>-1</sup> in acetonitrile. In the case of neutral reactants, intermediate and product, relatively small stabilizations occur but in the case of transition states and zwitterionic intermediates, larger solvation effects are observed due to increased charge separation. By lowering the energies of TSs, the activation energy of each elementary step become lower and thus make the reaction faster in solvent medium. For example, the  $\Delta E_{ZPE}^\ddagger$  for the rate-limiting step of the reaction path through the C=O bond addition with NH<sub>3</sub> is lower by 2.16 and 3.70 kcal mol<sup>-1</sup> in benzene

and acetonitrile, respectively, than in the gas phase. Similar stabilizations (1.95 kcal mol<sup>-1</sup> in benzene and 3.39 kcal mol<sup>-1</sup> in acetonitrile) also occur for the reaction path through the C=C bond addition. However, the reaction mechanism favoring the C=O addition to the C=C addition is still hold even in solution-phase, *i.e.*,  $\delta\Delta E_{ZPE}^\ddagger$  [ $=\Delta E_{ZPE}^\ddagger$  (C=C) -  $\Delta E_{ZPE}^\ddagger$  (C=O)], are 8.47 (gas phase), 8.68 (benzene) and 8.78 (acetonitrile) kcal mol<sup>-1</sup> for NH<sub>3</sub> addition.

The magnitude of solvation energies for the reaction with the dimeric (NH<sub>3</sub>)<sub>2</sub> in solutions is much greater than those with monomeric NH<sub>3</sub>. But such a large solvent effect cannot change the reaction mechanisms favoring the C=O addition, *i.e.*,  $\delta\Delta E_{ZPE}^\ddagger$  are +3.77 and +2.31 kcal mol<sup>-1</sup> in benzene and acetonitrile, respectively. As is well known, introduction of the secondary ammonia in the reaction decreases the activation barriers of all the reaction steps. However this phenomenon is more pronounced in the case of higher dielectric constant medium, acetonitrile. For example, decrease in the activation barrier by catalytic NH<sub>3</sub> molecule amounts to -19.72 (gas phase), -22.97 (benzene) and -24.71 (acetonitrile) kcal mol<sup>-1</sup>. This indicates that the solvent effects on the  $\Delta E_{ZPE}^\ddagger$  are larger for reactions with (NH<sub>3</sub>)<sub>2</sub> than those with NH<sub>3</sub>.

## Conclusions

*Ab initio* and hybrid density functional method calculations were performed to study both the un-catalyzed and catalyzed reaction mechanism of ketene with NH<sub>3</sub> and the dimer (NH<sub>3</sub>)<sub>2</sub>, respectively, in the gas phase and in benzene and acetonitrile solvent using 6-31+G(d,p) or 6-311+G(3df, 2p) basis set.

The following conclusions are the same as discovered by other researchers; (i) The pathway leading to the addition to the C=O bond requires lower activation barrier than that to addition to the C=C bond regardless of solvation. (ii) The catalyzed amination is more facile than the un-catalyzed one.

However the detailed mechanisms are quite different from those reported previously. In the gas phase catalyzed reaction, zwitterion **I(d)** is identified as a transient intermediate by IRC calculations and three transition structures, **TS1(d)**, **TS2(d)** and **TS4(d)**, are required to generate complete PES. **I(m)** in acetonitrile and **I(d)** in benzene are located as energy minima but become unstable or less stable when the ZPE correction is applied to the electronic energies. However, **I(d)** in acetonitrile is identified as a genuine minimum and should be included in mechanistic consideration.

From the complete PES for the amination reactions found from this work, we can conclude that the rate-determining step for the un-catalyzed reaction is breakdown of enol amide, **II(m)**, *via* **TS4(m)** but the rate-determining step for the catalyzed reaction is formation of **II(d)** *via* **TS2(d)**, which is opposite to the previous results. Therefore, the interpretation based on earlier works should be modified and reexamined. In order to consider this in detail, more thorough calculations are in progress in this lab.

**Acknowledgments.** This work was supported by the Brain Korea 21 Program. Professor C. K. Kim acknowledges Professor S. Wolfe (Simon Fraser University) for a careful editing of the manuscript.

### References and Notes

- (a) *The Chemistry of Ketenes, Allenes, and Related Compounds*; Patai, S., Ed.; John Wiley and Sons: New York, 1980. (b) Tidwell, T. T. *Ketenes*; John Wiley and Sons: New York, 1995. (c) Egle, I.; Lai, W.-Y.; Moore, P. A.; Renton, P.; Tidwell, T. T.; Zaho, D.-c. *J. Org. Chem.* **1997**, *61*, 18. (d) Butkovskaya, N. I.; Manke, G., II; Sester, D. W. *J. Phys. Chem.* **1995**, *99*, 11115. (e) Zhao, D.-C.; Allen, A. D.; Tidwell, T. T. *J. Am. Chem. Soc.* **1993**, *115*, 10097. (f) Tidwell, T. T. *Acc. Chem. Res.* **1990**, *23*, 273. (g) Allen, A. D.; Tidwell, T. T. *J. Am. Chem. Soc.* **1987**, *109*, 2774.
- (a) Duan, X.; Page, M. *J. Am. Chem. Soc.* **1995**, *117*, 5114. (b) Nguyen, M. T.; Sengupta, D.; Raspoet, G.; Vanquickenborne, L. G. *J. Phys. Chem.* **1995**, *99*, 11883. (c) Skancke, P. N. *J. Phys. Chem.* **1992**, *96*, 8065. (d) Nguyen, M. T.; Hegarty, A. F. *J. Am. Chem. Soc.* **1984**, *106*, 1552.
- (a) Lillford, P. J.; Satchell, D. P. N. *J. Chem. Soc. B* **1970**, 1016. (b) Lillford, P. J.; Satchell, D. P. N. *J. Chem. Soc. B* **1968**, 54.
- Lee, I.; Song, C. H.; Uhm, T. S. *J. Phys. Org. Chem.* **1988**, *1*, 83.
- (a) Sung, K.; Tidwell, T. T. *J. Am. Chem. Soc.* **1998**, *120*, 3043. (b) Wagner, B. D.; Arnold, B. R.; Brown, G. S.; Luszytk, J. *J. Am. Chem. Soc.* **1998**, *120*, 1827. (c) de Lucas, N. C.; Netto-Ferreira, J. C.; Androas, J.; Luszytk, J.; Wagner, B. D.; Scaiano, J. C. *Tetrahedron Lett.* **1997**, *38*, 5147. (d) Androas, J.; Kresge, A. J. *J. Am. Chem. Soc.* **1992**, *114*, 5643. (e) Seikaly, H. R.; Tidwell, T. T. *Tetrahedron* **1986**, *42*, 2587.
- Raspoet, G.; Nguyen, M. T.; Kelly, S.; Hegarty, A. F. *J. Org. Chem.* **1998**, *63*, 9669.
- (a) Briody, J. M.; Satchell, D. P. N. *Tetrahedron* **1966**, *22*, 2649. (b) Lillford, P. J.; Satchell, D. P. N. *J. Chem. Soc. B* **1967**, 360.
- The rate constants for the reaction of  $\text{PhMe}_2\text{SiCH}=\text{C}=\text{O}$  with amines in  $\text{CH}_3\text{CN}$  showed a mixed second- and third-order dependence on [amine]. See Allen, A. D.; Tidwell, T. T. *J. Org. Chem.* **1999**, *64*, 266.
- (a) Wolfe, S.; Kim, C.-K.; Yang, K.; Weinberg, N.; Shi, Z. *J. Am. Chem. Soc.* **1995**, *117*, 4240. (b) Wolfe, S.; Shi, Z.; Yang, K.; Ro, S.; Weinberg, N.; Kim, C.-K. *Can. J. Chem.* **1998**, *76*, 114.
- (a) Wolfe, S.; Kim, C.-K.; Yang, K. *Can. J. Chem.* **1994**, *72*, 1044. (b) Wolfe, S.; Ro, S.; Kim, C.-K.; Shi, Z. *Can. J. Chem.* **2001**, *79*, 1238. (c) Wolfe, S.; Akuche, C.; Ro, S.; Wilson, M.-C.; Kim, C.-K.; Shi, Z. *Can. J. Chem.* **2003**, *81*, 915. (d) Diaz, N.; Suárez, D.; Sordo, T. L. *J. Org. Chem.* **1999**, *64*, 3281. (e) Lopez, R.; Menendez, M. I.; Diaz, N.; Suárez, D.; Campomanes, P.; Sordo, T. L. *Recent Research Developments in Physical Chemistry* **2000**, *4*, 157.
- (a) Onsager, L. *J. Am. Chem. Soc.* **1938**, *58*, 1486. (b) Miertus, S.; Tomasi, J. *Chem. Phys.* **1982**, *65*, 239. (c) Foresman, J. B.; Keith, T. A.; Wiberg, K. B.; Snoonian, J.; Frisch, M. J. *J. Phys. Chem.* **1996**, *100*, 16098.
- (a) Liptak, M. D.; Gross, K. C.; Seybold, P. G.; Feldgus, S.; Shields, G. C. *J. Am. Chem. Soc.* **2002**, *124*, 6421. (b) Ilieva, S.; Galabov, B.; Musaev, D. G.; Morokuma, K.; Scharfer III, H. F. *J. Org. Chem.* **2003**, *68*, 1496.
- (a) Barra, M.; Fisher, T. A.; Cernigliaro, G. J.; Sinta, R.; Scaiano, J. C. *J. Am. Chem. Soc.* **1992**, *114*, 2630. (b) Chelain, E.; Goumont, R.; Hamon, L.; Parlier, A.; Rudler, M.; Rudler, H.; Daran, J.-C.; Vaissermann, J. *J. Am. Chem. Soc.* **1992**, *114*, 8088. (c) Qiao, G. G.; Androas, J.; Wentrup, C. *J. Am. Chem. Soc.* **1996**, *118*, 5634.
- (a) Wagner, B. D.; Zgierski, M. Z.; Luszytk, J. *J. Am. Chem. Soc.* **1994**, *116*, 6433. (b) Lippert, T.; Koskelo, A.; Stoutland, P. O. *J. Am. Chem. Soc.* **1996**, *118*, 1551.
- Palomo, C.; Cossio, F. P.; Cuevas, C.; Lecea, B.; Mielgo, A.; Román, P.; Luque, A.; Martinez-Ripoll, M. *J. Am. Chem. Soc.* **1992**, *114*, 9360.
- Visser, P.; Zuhse, R.; Wong, M. W.; Wentrup, C. *J. Am. Chem. Soc.* **1996**, *118*, 12598.
- Wang, J.-L.; Toscano, J. P.; Platz, M. S.; Nikolaev, V.; Popic, V. *J. Am. Chem. Soc.* **1995**, *117*, 5477. (b) Androas, J.; Chiang, Y.; Huang, C.-G.; Kresge, A. J.; Scaiano, J. C. *J. Am. Chem. Soc.* **1993**, *115*, 10605. (c) Barra, M.; Fisher, T. A.; Cernigliaro, G. J.; Sinta, R.; Scaiano, J. C. *J. Am. Chem. Soc.* **1992**, *114*, 2630. (d) Boate, D. R.; Johnston, L. J.; Kwong, P. C.; Lee-Ruff, E.; Scaiano, J. C. *J. Am. Chem. Soc.* **1990**, *112*, 8858.
- (a) Qiao, G. G.; Androas, J.; Wentrup, C. *J. Am. Chem. Soc.* **1996**, *118*, 5634. (b) Visser, P.; Zuhse, R.; Wong, M. W.; Wentrup, C. *J. Am. Chem. Soc.* **1996**, *118*, 12598. (c) Chelain, E.; Goumont, R.; Hamon, L.; Parlier, A.; Rudler, M.; Rudler, H.; Daran, J.-C.; Vaissermann, J. *J. Am. Chem. Soc.* **1992**, *114*, 8088.
- Barone, V.; Cossi, M. *J. Phys. Chem. A* **1998**, *102*, 1995.
- OPT=LOOSE option was used to achieve convergence in the optimization of *o*-nitrophenoxide using CPCM continuum solvation method. See Liptak, M. D.; Gross, K. C.; Seybold, P. G.; Feldgus, S.; Shields, G. C. *J. Am. Chem. Soc.* **2002**, *124*, 6421.
- Frisch, M. J.; Trucks, G. W.; Schlegel, H. B.; Scuseria, G. E.; Robb, M. A.; Cheeseman, J. R.; Zakrzewski, V. G.; Montgomery, J. A. Jr.; Stratmann, R. E.; Burant, J. C.; Dapprich, S.; Millam, J. M.; Daniels, A. D.; Kudin, K. N.; Strain, M. C.; Farkas, O.; Tomasi, J.; Barone, V.; Cossi, M.; Cammi, R.; Mennucci, B.; Pomelli, C.; Adamo, C.; Clifford, S.; Ochterski, J.; Petersson, G. A.; Ayala, P. Y.; Cui, Q.; Morokuma, K.; Malick, D. K.; Rabuck, A. D.; Raghavachari, K.; Foresman, J. B.; Cioslowski, J.; Ortiz, J. V.; Stefanov, B. B.; Liu, G.; Liashenko, A.; Piskorz, P.; Komaromi, I.; Gomperts, R.; Martin, R. L.; Fox, D. J.; Keith, T.; Al-Laham, M. A.; Peng, C. Y.; Nanayakkara, A.; Gonzalez, C.; Challacombe, M.; Gill, P. M. W.; Johnson, B.; Chen, W.; Wong, M. W.; Andres, J. L.; Head-Gordon, M.; Replogle, E. S.; Pople, J. A. *Gaussian 98, Revision A.6*; Gaussian, Inc.: Pittsburgh, PA, 1998.
- Gonzalez, C.; Schlegel, H. B. *J. Phys. Chem.* **1990**, *94*, 5523.
- (a) Carpenter, J. E.; Weinhold, F. *J. Mol. Struct. (Theochem)* **1988**, *169*, 41. (b) Reed, A. E.; Curtiss, L. A.; Weinhold, F. *Chem. Rev.* **1988**, *88*, 899.
- Similar charge separations were found for the corresponding group charges (in electrons) at B3LYP methods. B3LYP/6-31+G(d,p) level: -0.451 and -0.017 for the separated reactants and -0.700 and +0.402 for **II(d)**. B3LYP/6-31+G(3df,2p) level: -0.449 and -0.008 for the separated reactants and -0.700 and +0.399 for **II(d)**.
- Lee, I.; Kim, C. K.; Li, H. G.; Lee, B.-S.; Lee, H. W. *Chem. Phys. Lett.* **2000**, *320*, 307.
- Isaacs, N. *Physical Organic Chemistry*, 2<sup>nd</sup> ed.; Longman Scientific and Technical: Harlow, 1995; p 118.
- Boys, S. F.; Bernardi, F. *Mol. Phys.* **1970**, *19*, 553. (b) Jansen, H. B.; Ros, P. *Chem. Phys. Lett.* **1969**, *3*, 140.
- Wolfe, S.; Shi, Z.; Yang, K.; Ro, S.; Weinberg, N.; Kim, C.-K. *Can. J. Chem.* **1998**, *76*, 114.
- Kestner, N. R.; Combariza, J. E. *Reviews in Computational Chemistry*; Lipkowitz, K. B.; Boyd, D. B., Eds.; Wiley-VCH: New York, 1999; chap. 2.
- The data have been taken from the NIST Chemistry Webbook (<http://www.webbook.nist.gov>). We used the following heats of formations:  $\text{CH}_2=\text{C}=\text{O}$ : -14.78 kcal mol<sup>-1</sup>,  $\text{NH}_3$ : -10.97 kcal mol<sup>-1</sup>,  $\text{CH}_3-\text{C}(=\text{O})\text{NH}_2$ : -56.96 kcal mol<sup>-1</sup>.